Fibers and Polymers 2015, Vol.16, No.2, 245-253
DOI 10.1007/s12221-015-0245-0

ISSN 1229-9197 (print version)
ISSN 1875-0052 (electronic version)

Enhanced Bioactivity of Osteoblast-like Cells on Poly(lactic acid)/Poly(methyl methacrylate)/Nano-hydroxyapatite Scaffolds for Bone Tissue Engineering

Zhicheng Rong[†], Wen Zeng[1†], Yanshen Kuang[2], Jianwei Zhang[1], Xingyun Liu[3], Yuan Lu[3], and Xiangrong Cheng*

Key Laboratory for Oral Biomedical Engineering, Ministry of Education, School and Hospital of Stomatology, Wuhan University, Wuhan 430079, China
[1]*School of Resource and Environmental Science, Wuhan University, Wuhan 430079, China*
[2]*Zhongnan Hospital, Wuhan University, Wuhan 430079, China*
[3]*School of Chemistry and Chemical Engineering, Guangxi University, Nanning 530004, China*
(Received July 19, 2014; Revised September 18, 2014; Accepted September 29, 2014)

Abstract: Bone tissue engineering has great potential but requires an appropriate substrate with good bioactivity. In this study, poly(lactic acid) (PLA)/poly(methyl methacrylate) (PMMA)/nano-hydroxyapatite (n-HA) hybrid nanofibrous scaffolds were fabricated via electrospinning. The morphologies of the scaffolds were observed by scanning electron microscopy, transmission electron microscopy and the structures of the scaffolds were measured by fourier transform infrared spectrum. After immersion in simulated body fluid, the more deposition of ball-like apatite can be observed on the surface of the hybrid PLA/PMMA/n-HA scaffold. *In vitro* degradation experiments showed that the less degradation occurred in the hybrid PLA/PMMA/n-HA scaffold. The studies of cell adhesion and growth capability were investigated by incubating the osteoblast-like cells (MG-63) in the scaffolds, which verified the addition of n-HA could promote the adhesion and proliferation of the Human osteoblast-like cells (MG-63). Hence, the electrospun hybrid PLA/PMMA/n-HA nanofibrous scaffold is a promising biomaterial, propitious to be a substrate for bone tissue engineering.

Keywords: Hydroxyapatite nanoparticles, Nanofibrous scaffolds, Bioactivity, Bone tissue engineering

Introduction

Recently, scaffold based on bone reconstruction has been extensively investigated as a promising approach for bone tissue engineering [1]. One of the main driving forces to explore materials in bone engineering application is that bone defects have occurred in a wide variety of clinical cases, and the major therapeutic schedule for the problems are autografting or allografting, but even autografting suffers from supply shortage [2-4]. Bone tissue engineering combine bone scaffolds with osteoblasts, on the other hand, offers a new paradigm for treatment of skeletal defects. Some previous investigations by characterizing a wide range of pore diameter, high surface area to volume ratio, and morphological architectures, demonstrated that the 3D structure of fibrous scaffolds can enhance cells attachment, proliferation and differentiation [5,6]. In studies on osteoblasts, it was found that cells adhesion, proliferation, alkaline phosphatase activity and extracellular matrix production were increased through the use of thinner nanofibers [7].

Electrospinning is one of the most efficient methods that can be used to fabricate nanofibrous scaffolds with fiber diameter ranging from microns down to nanometers [8-11]. In comparison to other methods, such as drawing, template synthesis, phase separation and self-assembly, electrospinning is more economical, simpler and can yield more continuous and thinner fibers. And it is also versatile enough to spin both synthetic and natural polymers. Several materials can be mixed by solvents and were electrospun into hybrid scaffold as well as. What's more, highly porous three-dimensional (3D) electrospun fibers with aligned structures can be achieved by using various collectors, as well as conducting, oriented patterned substrates [12,13]. Therefore, electrospinning can be used to fabricate fibrous scaffolds for bone tissue engineering [14,15].

To optimize the mechanical and biomimetic properties of a fiber mesh, it is necessary to choose the appropriate materials. Since the PMMA was found to be a non-degradable biomaterial with good biocompatibility and mechanical properties, it has been widely used in bone cements, contact lenses and prosthetics. Studies showed that the mechanical properties of PMMA bone cement implanted for 15-24 years appeared to be comparable to freshly made PMMA, without indication of polymer deterioration [16]. Furthermore, it was reported that PMMA can be easily electrospun into nanofibrous films [17]. And addition of filler to PMMA is considered to be a potential method to improve its mechanical properties [18]. PLA is a biodegradable polymer material with good biocompatibility and widely applied for tissue engineering [19,20]. In some studies, PLA was incorporated in the bone tissue engineering scaffolds to improve their mechanical properties [20]. So the mixture of PLA and PMMA may have appropriate biodegradability and other properties better than PLA. The major constituent of natural bone is HA nanoparticles embedded in collagen matrix [1,21]. So the

[†]Co-first author with the same contribution to this work.
*Corresponding author: xiangrongcheng@hotmail.com

use of HA nanoparticles not only mimics the natural ECM but also is common in bone tissue engineering due to its bioactivity and osteoconductivity [22,23]. Furthermore, the incorporation of HA nanoparticles into polymer fibers can be easily achieved by convenient] blending of electrospinning method. Simultaneously, the electrospun composite fibers exhibit the distinctive properties with HA nanoparticles triumphantly incorporating and can even be expected exhibit improved properties over those of conventional fibers [24]. And that the addition of HA nanoparticles has been found to increase protein adsorption on these scaffold when compared to the conventional sized of HA particles [25]. It was reported that the presence of HA nanoparticles in scaffold could create a 3D microenvironment for better cellular interaction and proliferation [26,27]. Moreover, from a biological perspective, presence of HA enhances protein adsorption, improves osteoblast's function. As a matter of fact, there are several reports in regard to polymer-HA composite materials including blends of Collagen/HA, poly-l-lactic acid/HA and polyurethane/HA, which have been electrospun into fibrous scaffolds and their feasibility for bone tissue engineering have been proved [28-31].

Overall consideration, in this study, we attempt to disperse HA nanoparticles into PLA/PMMA blends and electrospinning them into composite fibrous scaffold. Series of characterizations have been carried out to testify bioactivity, biodegradation, cell adhesion and proliferation of PLA/PMMA/n-HA hybrid electrospun fibrous scaffold. Improved osteogenic capacity of these scaffold make it promising for bone tissue engineering.

Experimental

Materials

Poly(methyl methacrylate) (PMMA, M_w=120,000) was purchased from Alfa Aesar Co., USA. Poly(lactic acid) (PLA, M_w=238,000) was bought from Medical Polymer Institute (Shandong, China). Dichloromethane (DCM) and N,N-dimethylformamide (DMF) were used as a binary solvent system for dissolving PMMA and PLA. Hydroxyapatite (HA) nanoparticles with an average diameter of 20 nm were supplied by Emperor (Nanjing, China). In addition, Human osteoblast-like cells (MG-63, ATCC catalog CRL-1427) were obtained from American Type Culture Collection. All other chemical reagents were analytically pure or better.

Preparation of the Spinning Solutions

The blend of DMF and DCM with a volume ratio of 1:1 was used as solvents. An 8 % (w/v) PLA solution was obtained by dissolving PLA in the solvent with gentle magnetic stirring for 4 h. An 8 % (w/v) PMMA solution was obtained in a resemble way as PLA. PLA/PMMA mixed solution was prepared by mixing with 8 % (w/v) PLA and 8 % (w/v) PMMA. The PLA/PMMA/n-HA solutions were mixed at the same ratios of PLA/PMMA as above but containing 4 % HA nanoparticles. All solutions for electrospinning were prepared under stirring conditions.

Fabrication of Nanofibrous Scaffolds

The fabrication of nanofibrous scaffolds was similar to the previous report [32,33]. Briefly, the solution was fed into a 5 m*l* plastic syringe with a 6-gauge needle and continually driven by an advancing pump (SiLuGao Co. Beijing, China) at a speed of 2 m*l*/h. A DC voltage (BMei Co. Ltd., Beijing, China) of 20 kV was applied between the syringe needle and a grounded cylindrical collector with the tip-to-collector distance was 20 cm, and the collector was covered with aluminum foil. The ambient temperature and the relatively humidity were kept at 25 °C and 45 %, respectively. The electrospun fibers were dried under vacuum for a week to remove the residual solvents.

For culturing cells, the three as-spun nanofibrous membranes were cut into pieces of 15 mm×15 mm separately. The scaffolds pieces were washed with ethanol and de-ionized water for three times and added into Dulbecco's modified eagle medium (DMEM), respectively, and incubated at 37 °C for 24 h. Then they were disinfected with ethylene oxide and stored in vacuum at room temperature for further characterizations.

Characterizations

Scanning electron microscopy (SEM, Fei Quanta-200, Netherlands) was used to observe the morphology of the electrospun fibers. Transmission electron microscopy (TEM, Tecnai G2 20, Netherlands) was used to further study the dispersion of HA nanoparticles in the matrix. Fourier transform infrared spectra were recorded by a Nicollet 5700 spectrophotometer (Nicollet, Madison, USA).

In vitro Bioactivity and Biodegradation Studies

Soaking of Samples in SBF

The SBF solution was prepared by dissolving NaCl, $NaHCO_3$, KCl, $K_2HPO_4{\cdot}3H_2O$, $MgCl_2{\cdot}6H_2O$, HCl, $CaCl_2$, Na_2SO_4 and $(HOCH_2)_3CNH_2$ in ultrapure water, and ionic concentrations were similar to those in the inorganic part of human blood plasma [34], as shown in Table 1. Then buffered

Table 1. Several ionic concentrations (mM) of SBF and human blood plasma

Various ion	Na^+	K^+	Ca^{2+}	Mg^{2+}	HCO_3^-	Cl^-	HPO_4^{2-}	SO_4^{2-}
Blood plasma	142.0	5.0	2.5	1.5	27.0	103.0	1.0	0.5
SBF	142.0	5.0	2.5	1.5	4.2	147.8	1.0	0.5

at pH=7.40 with Tris-HCl buffer solution at room temperature. The samples were placed in glass vessels and soaked in 20 m*l* of SBF at 37 °C, respectively. The solutions were renewed every 2 days. The samples were taken out after 7 and 14 days, separately, and then washed with distilled water and dried by air for further characterization. The formation of n-HA layers on the surface of the scaffolds after immersion in SBF for 14 days was carried out by SEM and EDX (Quanta200, Philips) analysis.

In vitro Biodegradation Tests

The electrospun scaffolds were cut into rectangular sections (20 mm×20 mm) for degradation test. These rectangular membranes were weighed (W_0) and immersed in 15 m*l* phosphate buffer solution with pH of 7.4 at 37 °C. At different time intervals, samples were taken out from the incubator and blotted with filter paper to remove free water and weighed immediately (W_r). After that, washed and dried these samples in a vacuum oven and then weighed (W_s). The mass loss percentage (ML %) and water uptake percentage (WU %) of the membranes were calculated by the following formula accordingly:

$$ML\% = (W_0 - W_s) / W_0 \times 100 \quad (1)$$

$$WU\% = (W_r - W_0) / W_0 \times 100 \quad (2)$$

The differences of the degradation among different membranes were further investigated by using a SEM.

Cell Adhesion and Proliferation

MG-63 cells were cultured in DMEM supplemented with 10 % fetal bovine serum (FBS) at 37 °C in a humidified atmosphere where containing 5 % CO_2. The culture medium was renewed every three days. The cells were trypsinized and suspended when reached 80-90 % confluence. Cell count and viability were carried out using the Beckman-Coulter automatic cell counter (VI-cell analyzer, Beckman Coulter, Inc.). After that, they were seeded at a cell density of 1000 cells/cm^2.

Cell counting kit-8 (CCK-8; Dojindo Laboratories, Japan) was used to quantitatively analyze cell proliferation. After 1, 3, and 5 days of culture, PLA, PLA/PMMA and PLA/PMMA/n-HA fibrous membranes were gently washed with PBS and then 0.5 m*l* of DMEM containing 10 % CCK-8 was added per well. The disks were incubated at 37 °C for 3 h. The absorbance of supernatant was then measured at 450 nm using an ELX808 Ultra Microplate Reader (Bio-Tek Instruments, Inc., USA). The optical density values which reflected the viable cell populations were determined at least three times.

For the observation of cell skeleton, after 5 days' culture, cells were fixed using 3.7 % paraformaldehyde for 10 min, washed with PBS, and permeabilized with 0.1 % Triton X-100 solution for 5 min. The nonspecific binding sites were further blocked by incubating the coatings in PBS containing 1 % bovine serum albumin for 30 min. Filamentous actins (F-actins) were stained with rhodamine phalloidin (R-415 kit, Molecular Probes, Invitrogen, USA) for 20 min and nuclei were stained with 1:1000 2-(4-amidinophenyl)-6-indolecarbamidine dihydrochloride dilution (DAPI; Invitrogen, Basel, Switzerland) for 15 min at room temperature. After staining, the cells were washed with PBS and then stored in it. Immunofluorescence images were obtained using a Nikon TE-2000 inverted microscope. The fluorescence images with two colors were taken by double exposure with red light exposure first and blue next.

Statistical Analysis

All the *in vitro* cellular proliferation tests were performed triplicate, and data expressed as mean±standard deviation (SD). Multiple comparisons were done using one-way analysis of variance (ANOVA). The probability values of $p < 0.05$ were considered statistically significant.

Results and Discussion

Morphology of the Fibrous Mats

Figure 1 shows the morphology of the fabricated PLA, PLA/PMMA and PLA/PMMA/n-HA scaffolds. As we could see, the morphology of the nanofibrous membranes changed a lot when the PMMA was added into PLA, and the PLA/PMMA composite fibers became more compact and smooth compared with the pure PLA electrospun nanofibers. In Figure 1(a), some junctions among the pure PLA fibers, it can be seen that numerous randomly nanofibers interweave mutually into fibrous meshwork, which might be caused by the trace remained solvents after electrospinning [35]. PLA/PMMA nanofibers (Figure 1(b)) became more homogeneous compared with pure PLA nanofibers. Moreover, the diameters increased with the incorporation of the PMMA. At the same time, the SEM images of PLA/PMMA/n-HA composite electrospun nanofibers were shown in Figure 1(c), it was quite clear that a lot of n-HA particles were distributed into the fibers, besides, the fibers changed into roughness as HA nanoparticles was added into the PLA/PMMA mixtures. The former literatures demonstrated that surface property plays an important role in affecting the bioactivity, and suitable surface roughness may improve the bioactivity *in vitro* [36,37]. Thus, PLA/PMMA/n-HA composite electrospun nanofibers might exhibit better bioactivity.

For further investigation, TEM image of PLA/PMMA/n-HA composite nanofibers was presented in Figure 1(d), the HA nanoparticles with a diameter of 20 nm could be clearly exhibited and observed inset. These were in consistent with the results of the SEM image (Figure 1(c)), and directly confirmed the HA nanoparticles were successfully incorporated into the nanofibers.

FT-IR Spectra

Figure 2 shows the FT-IR spectra of pure PLA, pure PMMA, HA nanoparticles, PLA/PMMA hybrids, and PLA/

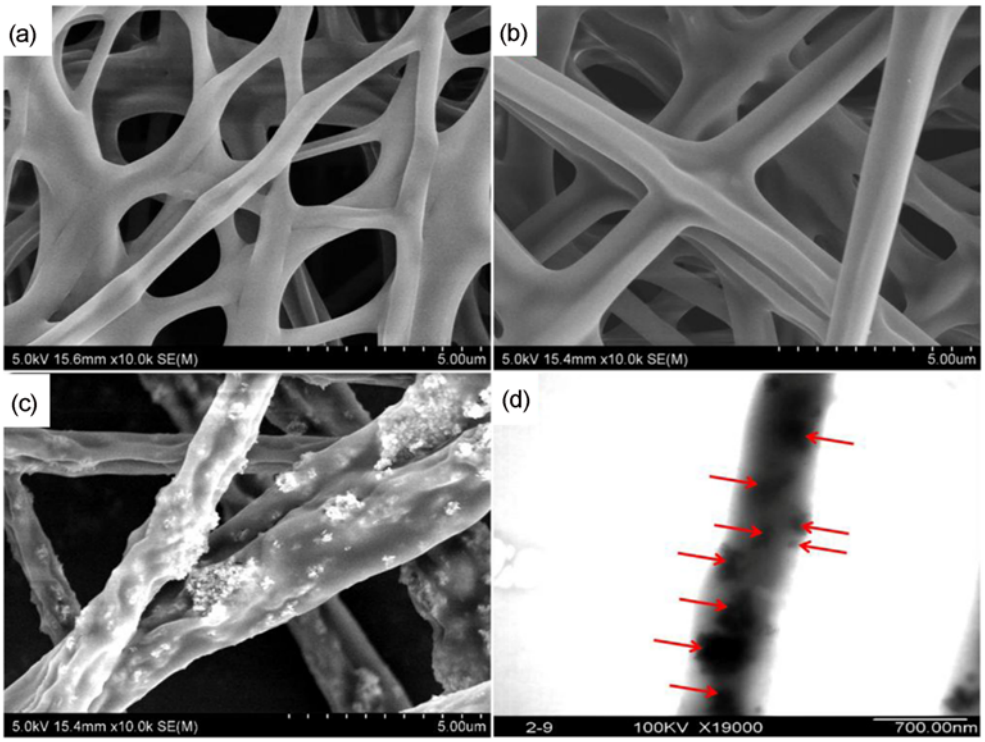

Figure 1. SEM images of electrospun scaffolds; (a) PLA, (b) PLA/PMMA, and (c) PLA/PMMA/n-HA. And TEM images of (d) PLA/PMMA/n-HA nanofiber.

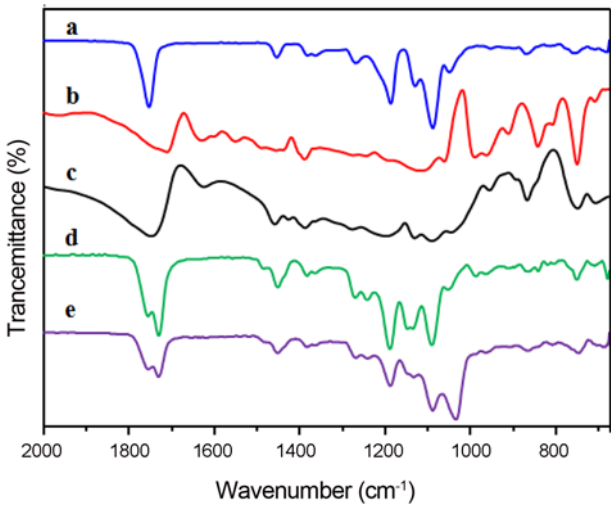

Figure 2. FT-IR spectra of (a) pure PLA scaffold, (b) pure PMMA scaffold, (c) HA nano-particles, (d) PLA/PMMA composite scaffold, and (e) PLA/PMMA/n-HA composite scaffold.

PMMA/n-HA composite scaffolds (Figures 2(a)-(d)), respectively. In the spectrum of pure PLA, the peak could be seen around 1753 cm^{-1} was attributed to C=O stretching vibration, and the peak around 1453 cm^{-1} was assigned to C-H deformation vibration. Peaks from C-O stretching vibration of PLA were at 1187 and 1090 cm^{-1} [38]. For the PMMA, it could be see that the peaks around 1771 and 1389 cm^{-1}, which were ascribed to the stretching vibration of C=O bonds and symmetric methyl CH_3 bending vibration. In the spectrum of PLA/PMMA, the sharp peak around 1750-1700 cm^{-1} was assigned to the stretching vibrations of the C=O group of PMMA and PLA, the multiple bands from 1250 to 1150 cm^{-1} are corresponding to the stretching vibration of C-O-C in PMMA. It could be speculated that, PLA and PMMA were mixed well. As shown in Figure 2, the spectrum of PLA/PMMA/n-HA composite nanofibrous scaffold was alike to that of PLA/PMMA, which might be due to overlap of the vibration bands of HA nanoparticles with those of PLA/PMMA within the scope of 2000 to 700 cm^{-1}. Certainly, slightly differences between the above two spectra could be distinguished, it could be seen that the peaks around 1150 cm^{-1} changed a lot in PLA/PMMA/n-HA composite scaffold compared to PLA/PMMA hybrid scaffold, which might be assigned to HA nanoparticles. What's more, one of the increased peaks around 1040 cm^{-1} appeared in PLA/PMMA/n-HA was attributed to the existence of PO_4^{3-} [24,39]. Hence, HA nanoparticles were successfully added into the fibers, which was in agreement with the results of TEM.

In vitro Bioactivity and Biodegradation Studies

In vitro Bioactivity Test

Apatite mineralization of bioactive materials is deemed to be a significant factor in chemical bonding between the

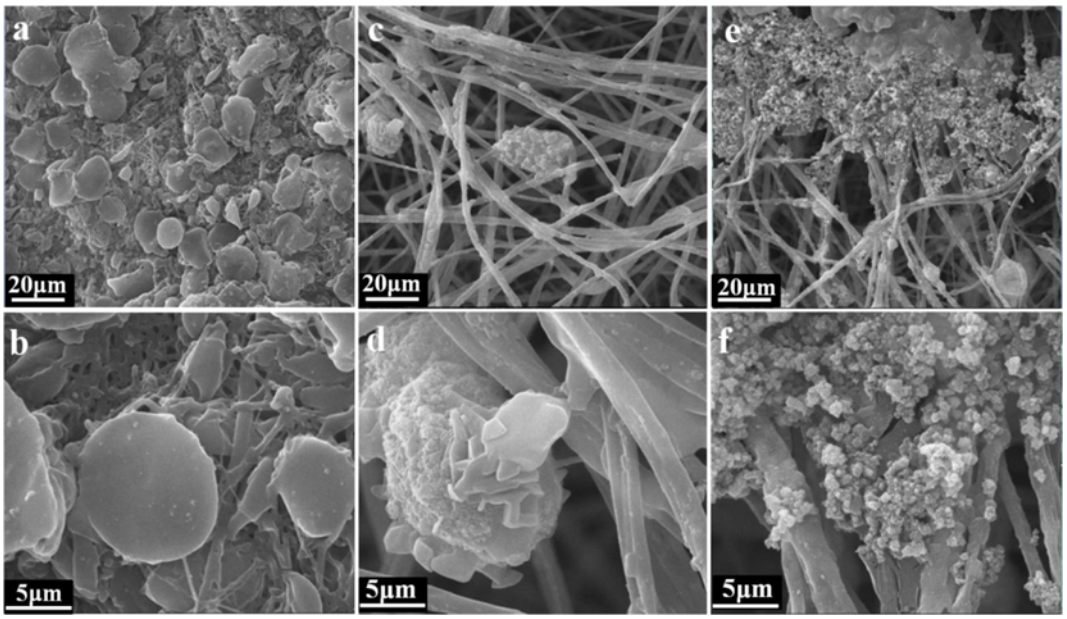

Figure 3. Morphology of the fibrous scaffolds soaked in SBF for 2 weeks: (a, b) PLA, (b, c) PLA/PMMA and (c, d) PLA/PMMA/n-HA.

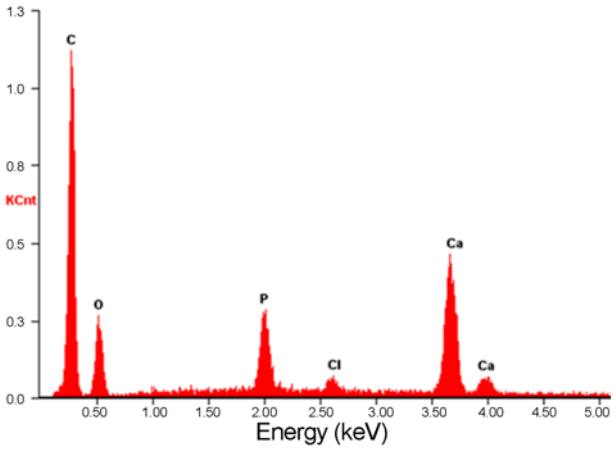

Figure 4. EDX spectrum of PLA/PMMA/n-HA composite fibrous scaffold after soaked in SBF for 2 weeks.

implant material and native bone tissue, thus affecting the *in vivo* success of bone grafting materials [40]. Figure 3 shows the surface morphology of electrospun fibrous membranes soaked into the SBF solution. It was obvious that quite a lot of spherical slices shaped crystallites were deposited on the surface of PLA membranes and covered the fibers very tightly (Figures 3(a) and (b)). As shown in Figures 4(c) and (d), a precipitated dune-like apatite layer made of a few spherical particles was covering on the composite PLA/PMMA fibers. With the presence of HA nanoparticles, a relative homogenous dense layer of infinitesimally small apatite particles of ball-like shape formed on the surface of the PLA/PMMA/n-HA composite scaffolds. Previous studies showed that materials possess ball-like apatite-formation ability and could release soluble ionic products to stimulate cell proliferation were highly bioactive [40,41]. Clearly, the addition of HA contributed to better bioactivity of the composite scaffold, and the result was in agreement with that of the SEM. EDX (Figure 4) results proved that the white layer formed on the surface of the fibers consists of Calcium and Phosphate elements, which were the components of the SBF solutions. What's more, the EDX analysis revealed the presence of chlorine element traces on the surface of the fibers, element rooted in the SBF solution. This *in vitro* test demonstrated that the PLA/PMMA/n-HA composite scaffold was more bioactive, and had potential for activate bone formation [41].

***In vitro* Biodegradation Test**

In vitro biodegradation of PLA, PLA/PMMA and PLA/PMMA/n-HA electrospun fibrous scaffolds were investigated in SBF solution for 5 weeks. All samples were biodegraded after long time dispersion in SBF solution. As seen in Figure 5(a), the differences in the mass loss of three nanofibrous scaffolds could be observed along with incubation time. Obviously, PLA fibers lost its mass almost linearly with immersion time and degraded more rapidly than both of PLA/PMMA fibers and PLA/PMMA/n-HA fibers, which suggested that the incorporation of PMMA increased the stability of fibers. Moreover, the PLA/PMMA/n-HA hybrid nanofibers showed a very slow degradation rate and a residual mass was not less than 97 % on the fifth week. Further investigation of those three scaffolds' biodegradation states was performed by SEM. Figure 6 exhibited very significant distinctions among those three scaffolds after 5 weeks

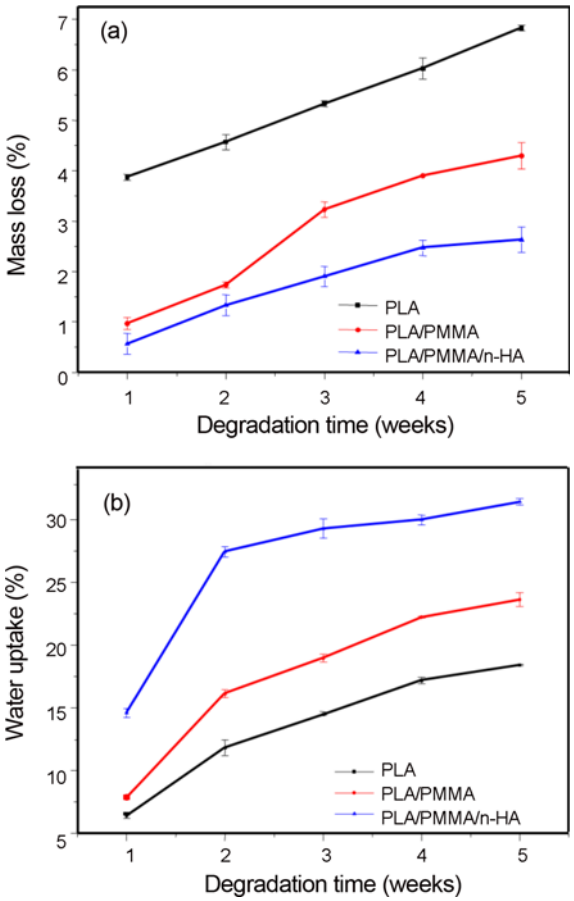

Figure 5. The weight loss percentage (a) and the water uptake percentage (b) of three kinds of electrospun scaffolds during the degradation process.

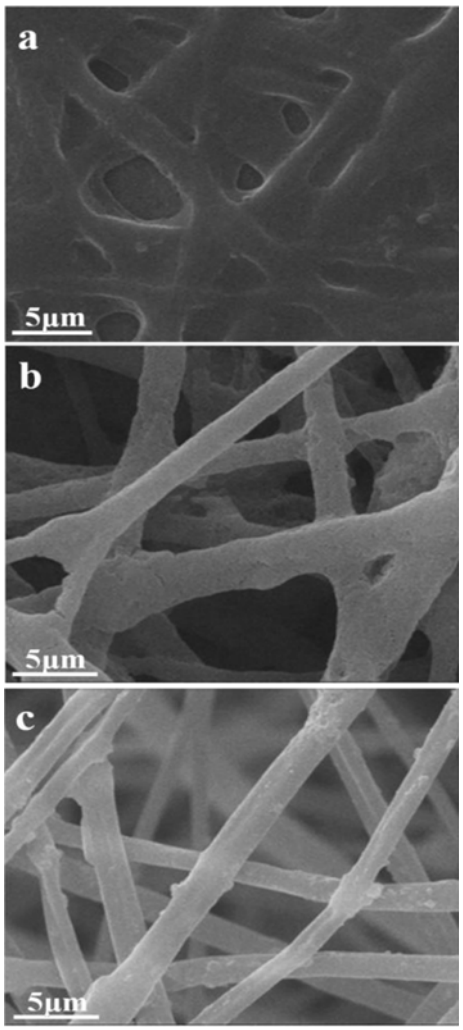

Figure 6. Morphology of electrospun fibers in PBS solution after 5 weeks of biodegradation period by SEM analysis (a) PLA, (b) PLA/PMMA, and (c) PLA/PMMA/n-HA.

biodegradation. PLA fibers (Figure 6(a)) were found to show dramatically morphological changes with uniform and smooth corrosion surface, while PLA/PMMA (Figure 6(b)) showed a certain degree of swelling and degradation. The fiber morphology of PLA/PMMA/n-HA (Figure 6(c)) composite fibrous scaffold appeared almost no changes meanwhile. It was reported that the corrosion pits of fibrous mats are homogeneous with nanophasic degradation patterns over a large scale [42]. Thus, the PLA/PMMA/n-HA electrospun nanofibrous scaffolds are suitable for bone tissue engineering. Though the degradation is beneficial to yield tissue integration and avoid subsequent surgical removal of scaffolds, and the rapid degradation would result in immediate loss of their electrical and mechanical properties, which might limit their long-term performance *in vitro* [43]. Therefore, PLA/PMMA/n-HA composite scaffolds with slower biodegradation rate are better for bone tissue engineering.

At the same time, wettability is also a very important property for biomaterials in tissue engineering, which has a great influence on the cell's adhesion, proliferation, and growth [44]. The water uptake percent of three scaffolds were measured in PBS. nd the results were exhibited in Figure 5(b), as degradation time went on, the water uptake percent of these three kinds of electrospun fibrous scaffolds was increased. In week 1, the water uptake percent of PLA, PLA/PMMA and PLA/PMMA/n-HA scaffolds were approximately 2, 3 and 14 %. And in week 5, the water uptake percent of PLA, PLA/PMMA and PLA/PMMA/n-HA scaffolds were approximately 18, 23 and 31 % separately. Therefore, the hydrophilcity of scaffolds improved with the addition of PMMA and HA nanoparticles.

In vitro Cell Adhesion and Proliferation

Cell attachment is the initial step in the process of tissue regeneration, as well as being a prerequisite for the growth of most human cells [45]. Therefore, electrospun scaffold should be effective to be attached by MG-63 cells that it could be applied for bone tissue engineering. In cell proliferation

on three kinds of scaffolds and was quantitatively assessed, thus, equal numbers of MG-63 cells were seeded on each scaffold. At the same time, a control was set during the course of this experiment. Figure 7 represents the time course for cell proliferation to various types of fibrous scaffolds. The absorbance value increased from day 1 to day 3 and day 5. But the control was exhibited highest absorbance value during the whole cell proliferation course. At day 1, no apparent difference was observed in cell proliferation among three kinds of scaffolds, but the amount of cell number was revealed increasing gradually for all samples. Generally, a higher cell number throughout the culture period was reached on PLA/PMMA/n-HA composite fibrous scaffolds compare to PLA and PLA/PMMA, indicated that this electrospun scaffold was more favorable for cell adhesion and growth. Additionally, the strength of adhesion to fibers was proven by cell trypsinization assay, and the results showed that osteoblast cells attached much more strongly onto PLA/PMMA/n-HA nanofibrous scaffold than the cells on other samples.

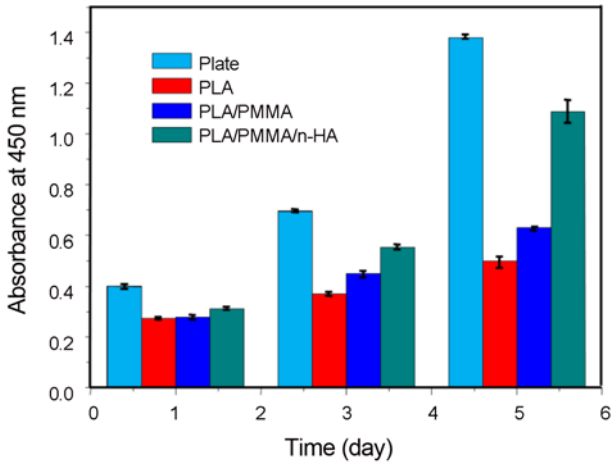

Figure 7. Proliferation of MG-63 cells in terms of absorbance index on electrospun scaffold PLA, PLA/PMMA, PLA/PMMA/n-HA after 1, 3 and 5 days of culture. Data are expressed as mean± SD.

Figure 8 shows that MG-63 cells adhered and proliferated better on PLA/PMMA/n-HA composite scaffold in day 5, the result is consistent with the result of cell proliferation test in Figure 7. Furthermore, cells exhibited pretty well shapes on PLA/PMMA/n-HA electrospun nanofibrous scaffold compared with the cells on the other two samples. Obviously, Previous researches indicated that it was very important to incorporate the nanosized components in engineered scaffolds in order to stimulate cell proliferation [46]. Consequently, the better adhesion and proliferation on PLA/PMMA/n-HA fibers might be attributed to the addition of HA nanoparticles.

Conclusion

In this study, PLA/PMMA/n-HA composite scaffolds were successfully prepared via electrospining. Good spinnability was demonstrated by SEM and TEM tests, moreover, PLA/PMMA/n-HA composite scaffold owned better fibers morphology. FT-IR results manifested that PLA and PMMA were well mixed and HA nanoparticles were successfully incorporated into the PLA/PMMA composite fibers. Wettability experiment demonstrated that the hydrophilic property of PLA/PMMA/n-HA composite nanofibers was better than that of the other two electrspun nanofibers. From the study on biodegradation of the scaffolds, PLA/PMMA/n-HA had a controllable and appropriate biodegradation rate. Apatite mineralization of electrospun scaffolds showed a relative homogenous dense layer of infinitesimally small apatite

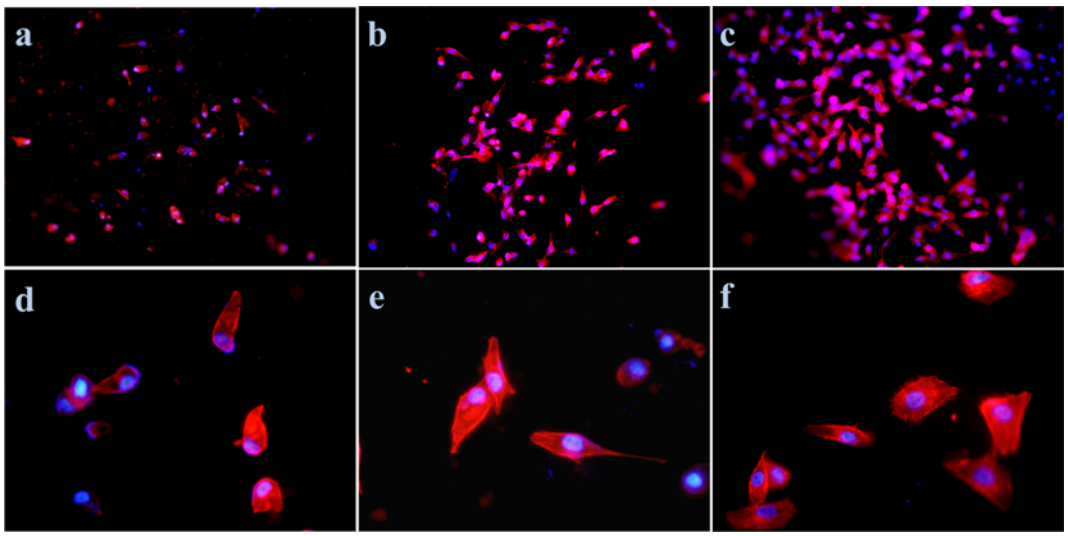

Figure 8. Confocal fluorescence images of MG-63 cells attached to (a, d) PLA, (b, e) PLA/PMMA and (c, f) PLA/PMMA/n-HA electrospun fibrous scaffolds after 5 days. The nuclei (blue) were stained with DAPI and F-actin (red) with radamine phalloidin.

particles of ball-like shape formed on the surface of the PLA/PMMA/n-HA composite scaffolds, and HA nanoparticles promoted the bioactivity of fibrous scaffold, thus, PLA/PMMA/n-HA equipped with better bioactivity. In addition, MG-63 cells seeded on PLA/PMMA/n-HA fibrous scaffolds exhibited significantly higher cell adhesion and proliferation ability compare to PLA and PMMA electrospun fibrous scaffolds. Hence, the PLA/PMMA/n-HA composite fibrous scaffold exhibited a great potential for bone tissue engineering.

Acknowledgments

This project was funded by National Natural Science Foundation of China (No.30772445).

References

1. A. K. Jaiswal, S. S. Kadam, V. P. Soni, and J. R. Bellare, *Appl. Surf. Sci.*, **268**, 477 (2013).
2. L. Tian, M. P. Prabhakaran, X. Ding, and S. Ramakrishna, *J. Biomater. Sci.-Polym. Ed.*, **24**, 1952 (2013).
3. M. Fröhlich, W. L. Grayson, L. Q. Wan, D. Marolt, M. Drobnic, and G. Vunjak-Novakovic, *Curr. Stem Cell Res. Ther.*, **3**, 254 (2008).
4. M. P. Prabhakaran, J. Venugopal, and S. Ramakrishna, *Acta Biomater.*, **5**, 2884 (2009).
5. W. J. Li, C. T. Laurencin, E. J. Caterson, R. S. Tuan, and F. K. Ko, *J. Biomed. Mater. Res. Part B*, **60**, 613 (2002).
6. S. L. Ishaug, G. M. Crane, M. J. Miller, A. W. Yasko, M. J. Yaszemski, and A. G. Mikos, *J. Biomed. Mater. Res. Part B*, **36**, 17 (1997).
7. T. J. Webster, R. W. Siegel, and R. Bizios, *Biomaterials*, **20**, 1221 (1999).
8. A. Frenot and I. S. Chronakis, *Curr. Opin. Colloid Interface Sci.*, **8**, 64 (2003).
9. J. Du, X. Li, C. Yang, W. Li, W. Huang, R. Huang, X. Zhou, and H. Deng, *Curr. Nanosci.*, **9**, 8 (2013).
10. Z. Ma, M. Kotaki, R. Inai, and S. Ramakrishna, *Tissue Eng.*, **11**, 101 (2005).
11. W. Huang, X. Li, Y. Xue, R. Huang, H. Deng, and Z. Ma, *Int. J. Biol. Macromol.*, **53**, 26 (2013).
12. X. Wang, B. Ding, G. Sun, M. Wang, and J. Yu, *Prog. Mater. Sci.*, **58**, 1173 (2013).
13. H. Deng, X. Zhou, X. Wang, C. Zhang, B. Ding, Q. Zhang, and Y. Du, *Carbohydr. Polym.*, **80**, 474 (2010).
14. Y.-F. Goh, I. Shakir, and R. Hussain, *J. Mater. Sci.*, **48**, 3027 (2013).
15. S. Liao, R. Murugan, C. K. Chan, and S. Ramakrishna, *J. Mech. Behav. Biomed. Mater.*, **1**, 252 (2008).
16. R. P. Chaplin, A. J. Lee, R. M. Hooper, and M. Clarke, *J. Mater. Sci.-Mater. Med.*, **17**, 1433 (2006).
17. H. Dong, V. Nyame, A. G. MacDiarmid, and W. E. Jones Jr., *J. Polym. Sci. Part B: Polym. Phys.,* **42**, 3934 (2004).
18. W. F. Mousa, M. Kobayashi, S. Shinzato, M. Kamimura, M. Neo, S. Yoshihara, and T. Nakamura, *Biomaterials*, **21**, 2137 (2000).
19. C. Wu, Y. Ramaswamy, Y. Zhu, R. Zheng, R. Appleyard, A. Howard, and H. Zreiqat, *Biomaterials*, **30**, 2199 (2009).
20. J. Yuan, J. Shen, and I. K. Kang, *Polym. Int.*, **57**, 1188 (2008).
21. P. Fratzl, H. S. Gupta, E. P. Paschalis, and P. Roschger, *J. Mater. Chem.*, **14**, 2115 (2004).
22. H. Yuan, Y. Li, J. De Bruijn, K. De Groot, and X. Zhang, *Biomaterials*, **21**, 1283 (2000).
23. K. L. Kilpadi, P. L. Chang, and S. L. Bellis, *J. Biomed. Mater. Res. Part B*, **57**, 258 (2001).
24. R. Nirmala, K. T. Nam, D. K. Park, W. Baek, R. Navamathavan, and H. Y. Kim, *Surf. Coat. Technol.*, **205**, 174 (2010).
25. C. Du, F. Z. Cui, X. D. Zhu, and K. de Groot, *J. Biomed. Mater. Res. Part B*, **44**, 407 (1999).
26. H.-W. Kim, J. C. Knowles, and H.-E. Kim, *Biomaterials*, **25**, 1279 (2004).
27. V. Thomas, D. R. Dean, M. V. Jose, B. Mathew, S. Chowdhury, and Y. K. Vohra, *Biomacromolecules*, **8**, 631 (2007).
28. R. L. Fischer, M. G. McCoy, and S. A. Grant, *J. Mater. Sci. Mater. Med.*, **23**, 1645 (2012).
29. R. J. Kane and R. K. Roeder, *J. Mech. Behav. Biomed. Mater.*, **7**, 41 (2012).
30. J. C. Antunes, J. M. Oliveira, R. L. Reis, J. M. Soria, J. L. Gomez-Ribelles, and J. F. Mano, *J. Biomed. Mater. Res. Part A*, **94**, 856 (2010).
31. H. Liu, L. Zhang, P. Shi, Q. Zou, Y. Zuo, and Y. Li, *J. Biomed. Mater. Res. Part B*, **95**, 36 (2010).
32. H. Deng, X. Li, B. Ding, Y. Du, G. Li, J. Yang, and X. Hu, *Carbohydr. Polym.*, **83**, 973 (2011).
33. W. Li, X. Li, W. Li, T. Wang, X. Li, S. Pan, and H. Deng, *Eur. Polym. J.*, **48**, 1846 (2012).
34. D. Rabadjieva, S. Tepavitcharova, K. Sezanova, R. Gergulova, R. Titorenkova, O. Petrov, and E. Dyulgerova, *Nanosci. Nanotechnol.*, **11**, 182 (2011).
35. H. Zhang, *J. Bioact. Compat. Polym.*, **26**, 590 (2011).
36. X. Hou, G. Yin, X. Chen, X. Liao, Y. Yao, and Z. Huang, *Appl. Surf. Sci.*, **257**, 3417 (2011).
37. H. Deng, X. Wang, P. Liu, B. Ding, Y. Du, G. Li, X. Hu, and J. Yang, *Carbohydr. Polym.*, **83**, 239 (2011).
38. R. C. Nagarwal, R. Kumar, M. Dhanawat, and J. K. Pandit, *Colloid Surf. B-Biointerfaces*, **86**, 28 (2011).
39. H. Cao, X. Chen, J. Yao, and Z. Shao, *J. Mater. Sci.*, **48**, 150 (2012).
40. C. Wu, J. Chang, S. Ni, and J. Wang, *J. Biomed. Mater. Res. Part A*, **76**, 73 (2006).
41. C. Wu, J. Chang, W. Zhai, S. Ni, and J. Wang, *J. Biomed. Mater. Res. Part B*, **78**, 47 (2006).
42. L. Mao, L. Shen, J. Niu, J. Zhang, W. Ding, Y. Wu, R. Fan, and G. Yuan, *Nanoscale*, **5**, 9517 (2013).

43. D. Kai, M. P. Prabhakaran, G. Jin, and S. Ramakrishna, *J. Biomed. Mater. Res. Part A*, **99**, 376 (2011).
44. H. Liu, S. Wang, and N. Qi, *J. Appl. Polym. Sci.*, **125**, E468 (2012).
45. B.-W. Chang, C.-H. Chen, S.-J. Ding, D. C.-H. Chen, and H.-C. Chang, *Sens. Actuators B-Chem.*, **105**, 159 (2005).
46. J. Pelipenko, P. Kocbek, B. Govedarica, R. Rošic, S. Baumgartner, and J. Kristl, *Eur. J. Pharm. Biopharm*., **84**, 401 (2012).